Sub-Hourly to Daily Rainfall Intensity-Duration-Frequency Estimation Using Stochastic Storm Transposition and Discontinuous Radar Data

Andersen, Christoffer B.; Wright, Daniel B.; Thorndahl, Søren

Published in:
Water (Switzerland)

DOI (link to publication from Publisher):
10.3390/w14244013

Publication date:
2022

Document Version
Publisher's PDF, also known as Version of record

water

MDPI

Article

Sub-Hourly to Daily Rainfall Intensity-Duration-Frequency Estimation Using Stochastic Storm Transposition and Discontinuous Radar Data

Christoffer B. Andersen [1,2,*], Daniel B. Wright [2] and Søren Thorndahl [1]

[1] Department of the Built Enviroment, Aalborg University, 9220 Aalborg East, Denmark
[2] Department of Civil and Envrionmental Engineering, University of Wisconsin-Madison, Madison, WI 53706, USA
* Correspondence: cband@build.aau.dk

Abstract: Frequency analysis of rainfall data is essential in the design and modelling of hydrological systems but is often statistically limited by the total observation period. With advances in weather radar technology, frequency analysis of areal rainfall data is possible at a higher spatial resolution. Still, the observation periods are short relative to established rain gauge networks. A stochastic framework, "*stochastic storm transposition*" shows great promise in recreating rainfall statistics from radar rainfall products, similar to rain gauge-derived statistics. This study estimates intensity–duration–frequency (IDF) relationships at both point and urban catchment scales. We use the stochastic storm transposition framework and a single high-resolution, 17-year long (however, discontinuous), radar rainfall dataset. The IDF relations are directly compared to rain gauge statistics with more than 40 years of observation, and rainfall extremes derived from the original, and untransposed, radar dataset. An overall agreement is discovered, however, with some discrepancies in short-duration storms due to scaling errors between gauge and radar.

Keywords: radar rainfall; extreme rainfall; rainfall frequency analysis

Citation: Andersen, C.B.; Wright, D.B.; Thorndahl, S. Sub-Hourly to Daily Rainfall Intensity-Duration-Frequency Estimation Using Stochastic Storm Transposition and Discontinuous Radar Data. *Water* **2022**, *14*, 4013. https://doi.org/10.3390/w14244013

Academic Editor: Francesco Cioffi

Received: 22 September 2022
Accepted: 5 December 2022
Published: 8 December 2022

1. Introduction

Frequency analysis of rainfall data is an invaluable tool in the field of hydrology. An intuitive understanding of the relations between rainfall intensity, storm duration, and return levels is beneficial to modelers and decision makers in performing risk assessments and to design complex hydraulic and hydrological structures/systems. These relations can be described as intensity–duration–frequencies (IDF), also sometimes referred to as depth–duration–frequencies, and are derived statistically from rainfall measurements, most commonly from different types of rain gauge networks [1,2]. These networks can capture regional variability in rainfall but are rarely so densely located that the derived statistics can account for the heterogeneity and chaotic nature of rainfall fields [3]. This lack of spatial information is considered a great source of error in hydrological modeling [3–7], where non-homogeneous land covers can result in vastly different runoff times and general complex runoff response. A fast runoff response especially challenges hydrological modeling of urban areas, and is, thus, critical to short (sub-hourly) rainfall durations with high intensity, complex flow structures, and requirements to avoid capacity exceedances for low return levels. Urban hydrological models, therefore, require rainfall input data in high spatial and temporal resolution to discretize the runoff processes sufficiently.

Major advancements in radar technology in the last few decades have enabled measurements of rainfall fields in higher resolution, both temporally and spatially. However, the novelty of weather radar limits the frequency analysis level one can perform, and any frequency analysis is limited by the total length of the observation period. IDF curves directly derived from radar data will most likely be associated with significant margins of

error compared to datasets with significantly more extended observation periods, such as rain gauges [8–11].

Extreme value rainfall statistics are traditionally derived either using the plotting position of ranked values of either an "*annual-maxima-series*" (AMS) [12] or "partial-duration-series" (PDS) (also referred to as *peaks-over-threshold*) [13,14] approach. The plotting position approach is severely limited by the observation period, i.e., the maximum return level that can be inferred is the total length of the data series (i.e., no extrapolation is possible). The AMS and PDS approaches sample values from the time series in two different ways. AMS samples maximum value in specified block sizes, usually calendar years, whereas PDS samples values above a specified threshold. The sampled values are fitted to a distribution function from which frequency analysis is performed.

The IDF curves display the relations between the duration of a rain event and the average rainfall intensity over this duration. IDF curves can be converted into design storms (Chicago-design storms or unit hyetographs [15,16]), allowing a response assessment of multiple storm durations and return levels.

To incorporate the spatial variability in rainfall, area reduction factors (ARF) are applied. The ARF describes the ratio areal rainfall and point rainfall for a specific rainfall duration. ARFs can be derived from rain gauge networks [17,18] or from radar data [11,19,20]. ARF can directly be applied to design storms (IDF values or CDS storms) to emulate the spatial variability of rainfall fields over a specific area. However, the process of deriving these ARF often neglects the several complexities that follow the chaotic nature of rainfall [21].

A stochastic framework, known as stochastic storm transposition (SST) [22,23], is an alternative approach to performing frequency analysis. This method virtually lengthens the period of record for the dataset in question by resampling rainfall in time and space. The method is applied and presented in Wright et al. [24,25] coupled with a "storm-catalog" approach (a selected number of storms, for specified rainfall durations, are pooled into a catalog), using rainfall products from the NEXRAD radar network [26]. The method shows great promise in replicating extreme-value rainfall statistics, comparable to rain gauge statistics, with return levels significantly longer than the observation period of the applied radar dataset. The analyses in Wright et al. [24,25] focused on long rainfall durations and high return levels (e.g., 100 years). For urban areas, shorter duration (sub-hourly) and more frequent (return levels $\leq$10 years) storms are of interest, as described earlier.

In this study, we estimate IDF values from different datasets: single rain gauges, a regional model (based on a network of rain gauges), and weather radar data. We use PDS sampling for both rain gauge and radar data, and the SST framework for the radar data, only. We then compare the output to examine the validity of the SST approach when using a different dataset in a different climatological location than applied in Wright et al. [24]. Even though this study broadly follows the concepts presented in Wright et al. [24], the novel contribution is applying the SST framework to a structurally different radar dataset, different climatological conditions, and validation through traditional statistical models at low return levels. The radar dataset we use in this study is structurally different from the one used in Wright et al. [24] by having a higher resolution, only stemmning from a single radar, and being discontinuous in time. The resolution of the radar product is of greater detail, relative to Wright et al. [24], both spatially and temporally, allowing for sub-hourly IDF estimates at both point and catchment scale. Therefore, one of the paper's objectives is to investigate whether the SST approach can be applied to estimate sub-hourly IDF estimates for urban catchment scales using rainfall estimates from a single radar covering 17 full years. Another objective is to study the relationship between data observation periods (for both rain-gauge and radar data) and the corresponding validity of the derived return levels, especially for return levels in the same order of magnitude as the observation periods or even larger ones. Subsequently, we investigate low return levels since the applied radar dataset should contain sufficient data for traditional frequency analysis to be performed and, thus, allow for more validation of the SST framework.

This paper is structured as follows: the overall study area and other necessary data are presented and discussed in Section 2; specifically, the different types of rainfall data, and pre-processing, are presented in Sections 2.2–2.4. Section 3 presents the applied methodologies, specifically: the background for stochastic storm transposition, Section 3.1, and discussion of hyperparameters, applied rainfall frequency analysis, Section 3.2 and areal reduction factors, Section 3.4. Sections 4.1 and 4.2 discuss crucial aspects of the SST framework; Section 4.3 shows IDF results for the radar/rain gauge dataset and the regional model, with point/pixel being highlighted in Section 4.4 and catchment scale IDF curves highlighted in Section 4.5. Lastly, Section 5 sums up the entire study, and final remarks are made.

2. Data and Study Area

2.1. Study Area

The island of Zealand in Denmark was chosen as a general study area, with the city of Copenhagen as a specific area of interest (AOI) (Figure 1).

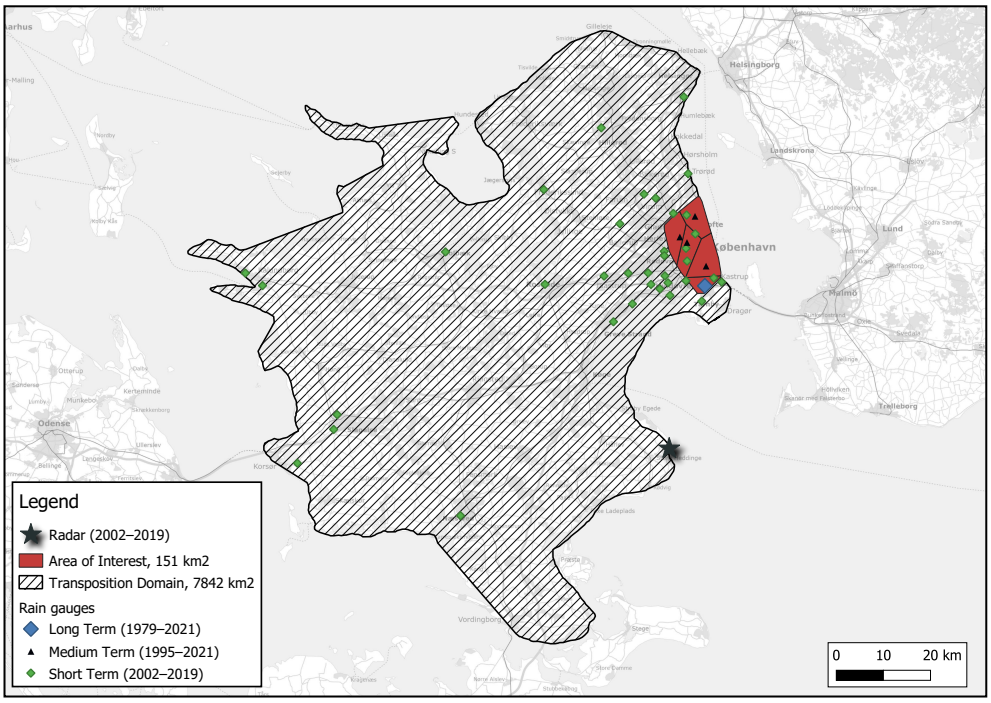

Figure 1. Island of Zealand: the study area for the present study. The shaded area represents the transposition domain used for the SST method, as presented in Section 3.1. All rain gauges used in the study are shown and labeled with the length of the observation period. The red area encapsulates the city of Copenhagen, which serves as the area of interest for the study. The division in the red-shaded area is a Voronoi polygon which is used to create area-weighted rainfall series.

The greater Copenhagen area is the largest urbanized area in Denmark and, therefore, the largest urban drainage system.

The Copenhagen area encompasses several meteorological measuring stations that are used to verify the results of the SST procedure. We utilize three different meteorological datasets in this study: rain gauges, Section 2.2; a regional rainfall model (derived from a national network of rain gauges), Section 2.3; and a single weather radar, Section 2.4.

2.2. Rain Gauges

The rain gauges we apply in this study are a part of a more extensive network of rain gauges managed by the Water Pollution Committee (WPC) [27] in Denmark. The network consists of tipping-bucket rain gauges which register rainfall with a resolution of 0.2 mm. Rainfall registrations are processed into time series with a temporal resolution of 1 min.

The measured rainfall intensities are grouped into single rainfall events. A rainfall event is triggered at the first registered tip and ends if no tip is recorded for 60 min. Events consisting of only one tip are discarded.

Rain-gauge data serves multiple purposes in this study. A single rain gauge (long term, 1979–2021), shown in Figure 1, is used to derive IDF values for rainfall events with durations of 10, 30, 180, 360, 720, and 1440 min and for return levels of 2, 5, 10 and 100 years, using a "*partial-duration-series*" approach (presented in Section 3.2). A collection of five rain gauges is used to estimate rainfall statistics at catchment scale for the selected area of interest (Figure 1). These gauges have the longest common period of record, of about 25 years (1995–2021), and are combined to one areal rainfall time series by applying an area-weighted average based on the area division (Voronoi polygons) presented in Figure 1. These gauges are referred to as the medium-term gauges. The final rain-gauge dataset covers the same period as the observed radar data (2002–2019) and consists of 37 rain-gauge stations spatially distributed over the whole domain. These gauges are referred to as the short-term gauges.

2.3. Regional Model

A regional extreme-value model (named the Danish regional rainfall model) for rainfall intensities, was developed by the WPC on the basis of a large collection of rain gauges (83 gauges, all with more than 10 years of data, collectively 1881 station years [28]). The presented rain gauges in Section 2.2 are a part of this collection. The output from the Danish regional rainfall model is IDF estimates at specified rainfall durations (10, 30, 180, 360, 720, 1440, and 2880 min, with interpolation available between these values). Parameters of a generalized Pareto distribution are modeled after regional rainfall data to investigate regional differences in extreme rainfall. The model is well-documented in Madsen et al. [1] and Gregersen et al. [29]. The regionalization makes the IDF estimates less sensitive to outliers, and different sources of errors [14]. Furthermore, the regionalization and distribution fit enables extrapolation of IDF estimates, so that return levels beyond the observation period can be inspected. The model evaluates IDF values at point-scale; hence, we choose to apply areal reduction factors, to the IDF values, to obtain an estimate at catchment scale. The derivation of these factors is presented in Section 3.4.

2.4. Radar Rainfall

We use data from a single weather radar as input to the SST framework. We also estimate IDF curves from a single pixel (same location as the long-term gauge in Figure 1) and at catchment scale (area of interest in Figure 1).

The radar is a C-band weather radar, located in south Copenhagen, as presented in Figure 1. The radar is operated by the Danish Meteorological Institute (DMI). For this study, data from 2002–2019 is available. From the raw radar scannings, a radar reflectivity product with a (pseudo) constant altitude of 1 km, a 10-minute temporal resolution, and a cartesian 500 m $\times$ 500 m spatial resolution is generated. The reflectivity is converted into rain intensities using a standard Z-R Marshall–Palmer relation [30]. To increase the precision of the radar-rainfall product, the radar data is daily mean-field bias-adjusted against rain gauges within the transposition domain (Figure 1). The complete processing of the radar dataset is documented in Thorndahl et al. [30] and applied in [9,20,31].

The temporal resolution is increased to 1 min using the advective interpolation methodology presented in Nielsen et al. [32] to improve the quality of the precipitation product further, as shown in Thorndahl et al. [30]. For computational purposes, the radar rainfall product used in this study is converted back to a 10-minute resolution maintaining the improved quality of the 1-minute product (not shown in this study).

For spatio-temporal radar data, it is challenging to define unambiguous rain events, as can be performed with rain gauge data (Section 2.2). Instead of defining events, the radar data is grouped into observation days, from midnight to midnight (00 UTC), containing both dry and wet periods. During the radar's observation period, there are different types of breakdowns, malfunctions, and problems, e.g., filtering ground clutter or external emitters.

Furthermore, rainfall days with poor-quality bias-adjustment due to too little rain-gauge data are removed from the dataset. This leaves the dataset discontinuous and somewhat inconsistent in time. In total, 1104 rainfall days (with more than 3 mm of rain anywhere in the domain) are considered to be of high enough quality to be included in this study. This corresponds to 65 rainfall days per year. In comparison, Thejll et al. [33] states that the average year has 117 days with more than 0 mm of rain. Since this discrepancy covers days with very little rainfall, it is not expected to impact the extreme-value statistics of this study.

3. Methods

3.1. Stochastic Storm Transposition

Performing frequency or extreme-value analysis on any dataset is limited by the total length of observation. To derive valid rainfall statistics beyond the period of observation of the applied radar dataset, we implement the stochastic framework "stochastic storm transposition". The procedure virtually extends the observation period by resampling the rainfall in time and space. It assumes that storms recorded in space are statistically independent and that there is an equal likelihood of storm occurrences in space (cf. the homogeneous climatology assumption). Furthermore, it is assumed that the frequency of storm occurrence at a point or at catchment scale is represented by the spatiotemporal information in the SST sampling domain over the observation period. The procedure is presented in detail in Wright et al. [24] and was later implemented in the open source python tool *RainyDay* [34], which is utilized in this study and other studies [35,36]. A brief explanation of the procedure is presented in the following, along with some *RainyDay* hyper-parameter choices and reflections.

1. We specify the island of Zealand (7842 km^2) as our transposition domain from which rainfall will be resampled, see Figure 1. A prerequisite/assumption for random transposition to the area of interest (151 km^2) is that the selected domain's extreme rainfall climatology is homogeneous. This assumption is assessed and discussed in Section 4.1.
2. The 500 largest storms at durations: 10, 30, 60, 180, 360, 720, and 1440 min are identified by ranking storms with the same shape and size as the area of interest (Figure 1). This collection of storms is henceforth known as the storm catalog (e.g., 60-minute storm catalog or simply 60-minute catalog). The creation of the storm catalogs is further described in Section 4.2.
3. The number of yearly storm occurrences for each duration is assumed to follow a Poisson distribution with a rate parameter: $\lambda = 88$ (average 88 storms per year). This derivation will be further explained in Section 4.2.
4. From the storm catalog in question (e.g., 60-min), we randomly select a storm. The assumption of homogeneous climatology, within the transposition domain, allows us to stochastically transpose the series of radar images in the x, y directions, since the storm is assumed to have equal likelihood to have appeared anywhere within the domain. Every time step of the radar image series is transposed with the same vector, so the original motion of a rain storm is retained, and only the spatial occurrence is altered.
5. Step 4 is repeated k times where k is a random integer drawn from the Poisson distribution explained in step 3. The k storms represent one year of rainfall.
6. For each transposed storm in step 4, we compute the t-minute catchment-average/point rainfall depth, for the area/point of interest.
7. Steps 4–6 are repeated 1000 times to create 1000 years of synthetic storm events. The 1000 largest values from all of the synthetic years are retained (following a general "*partial-duration-series*" approach), and IDF values are estimated.
8. Steps 4–7 are repeated, for this study, 100 times to quantify the uncertainty of the estimated IDF values.

In this study, we switch from the default frequency estimate of AMS in RainyDay to the PDS approach. This is carried out to make the results more comparable to the IDF curves derived from the rain gauge and the WPC regional model. Madsen et al. [14] show

that the PDS approach provides a more accurate frequency analysis than the AMS approach for short rainfall durations.

To relate this study to urban drainage design practice, the examined return levels are chosen to be: 2, 5, 10, and 100 years. These are typical values applied in Danish urban-drainage design and analysis for estimating system capacity exceedance at different service levels [37].

Two ensembles of storms are generated from the RainyDay tool. One SST ensemble is based on a point of interest. IDF statistics are derived for a single radar pixel which is directly compared to the same point in the WPC regional model and the empirical IDF statistics of the long record rain gauge, as seen in Figure 1. These different ways of estimating IDF relationships will function as a validation of the SST framework for point rainfall IDF statistics. The second SST ensemble is at catchment scale and developed specifically for the area of interest presented in Figure 1. SST IDF statistics derived from the catchment storm catalog are compared to spatially weighted averaged IDF statistics of the rain gauges within the area of interest and to the WPC regional model with areal reduction factors applied.

3.2. Rainfall Statistics

Return levels for mean rainfall intensities across the selected durations (10, 30, 60, 180, 360, 720, and 1440 min) are estimated in two ways: (1) empirically by plotting position; thus, by estimation of return levels by the ranking, in descending order, of storms (Equation (1)); and (2) by extreme-value analysis, where data is fitted to a generalized Pareto distribution (GPD) following Madsen et al. [1] (Equation (2)). For both methods, the PDS approach is used. A key factor in the PDS approach is the selection of a threshold value for the exceedance of intensities for a given duration. This value should be low enough for a meaningful extreme-value analysis to be performed while allowing the selected data points to follow the GDP distribution. Following the recommendation from Gregersen et al. [29], the threshold value is chosen so that we observe, on average, three exceedances per year ($\lambda_{PDS} = 3$ yrs^{-1} in Equation (2)). Similar approaches are used in [1,29,31].

The return levels are estimated empirically by the California plotting position method (Equation (1)):

$$T = \frac{N}{rank} \tag{1}$$

where T denotes the return level of the specified rainfall intensity over a given duration, N is the total length of observations, and *rank* is the rank position of the sorted rainfall intensities.

For the short-term observations (rain gauge and radar data), an extreme-value analysis is performed to estimate return levels larger than the observation period. We use the GDP distribution to estimate return levels (inverse exceedance probability) which, in its reformulated state, is presented in Equation (2) [38]:

$$z(T) = z_0 - \frac{\beta}{\gamma}\left[1 - \left(\frac{1}{\lambda_{PDS}T}\right)^{-\gamma}\right] \tag{2}$$

In which $z(T)$ is the rainfall intensity for return level T, z_0 is the threshold value, an β and γ are the shape and scale parameters of the GPD. The scale and shape parameters are estimated with maximum likelihood (MLE) optimization. An individual fit of the GDP distribution is performed for each chosen rainfall duration. Uncertainty of the modelled extreme values, for each of the investigated rainfall durations, $z(T)$, is obtained through Equation (3) [38]:

$$Var(z(T)) = \left(\frac{\partial\beta}{\partial z}\right)^2 Var(\beta) + \left(\frac{\partial\gamma}{\partial z}\right)^2 Var(\gamma) \tag{3}$$

3.3. Pixel-Scale Duration Bias

Our study investigates extreme rain rates at the sub-hourly scale (10- and 30-min duration). At these time scales, a significant bias between radar rainfall product and gauge-

based ones are to be expected (both observed in Peleg et al. [39] and [20,30,31] for the applied dataset). We examine this bias through (4) similar to Thorndahl et al. [20].

$$B(d) = \frac{\sum_{t=1}^{T}\left(\sum_{n=1}^{N} G_{max}(n,d)\right)}{\sum_{t=1}^{T}\left(\sum_{n=1}^{N} R_{max}(n,d)\right)} \quad (4)$$

where $B(d)$ denotes the duration (d)-specific bias. $G_{max}(n,d)$ and $R_{max}(n,d)$ is the daily duration specific maximum intensity for co-located gauge/pixel pairs (n), N being total number of pairs and T being the total number of days with radar data (1104 for this study).

3.4. Areal Reduction Factors

The regional model, WPC, presented in Section 2.3, only evaluates IDF estimates at point scale. Estimating areal values is, thus, achieved by multiplying areal reduction factors (ARF) directly to WPC model point rain intensities. The ARF model is developed in Thorndahl et al. [20] using the same radar dataset as used in this study. The ARF values are derived using a storm-centered approach and fitted to a three-parameter model, as presented in Thorndahl et al. [20]:

$$ARF = \exp\left(\frac{-0.31A^{0.38}}{d^{0.26}}\right) \quad (5)$$

In which A [km^2] denotes the areal coverage of rainfall (in this case, the area of interest in Figure 1 and d (min) is the storm duration. For the area of interest of 151 km^2, this equals an ARF of 0.49 for a 60-min storm duration.

4. Results and Discussion

4.1. Transposition Domain Selection and Assessment

Two references justify the assumption of the climatological homogeneity of the transposition domain: (1) with regards to annual precipitation in [33,40] in which the average precipitation is reported to vary from 615 mm (in the south of the domain) to 675 mm (in the north of the domain) per year (average 1981–2010); thus, a variability of less than 10%; and (2) by the extreme-value distribution in WPC regional model Madsen et al. [28] in which no significant difference in the regional rainfall estimates of 60 min at a 10-year return level (24 mm) is reported, and a minor variability at 1440 min (1 day) regional rainfall estimates at the 10-year return level of 57 $\pm$ 4 mm. In general, Madsen et al. [28] report variability of up to 10% at different return levels and durations between the north and south of the island of Zealand. Due to this relatively low variability, the assumption of climatological homogeneity is considered to be met. Consequently, we can apply a uniform storm transposition scheme within the domain.

4.2. Rainfall Catalog Creation

A core concept in the SST framework is to create duration-specific rainfall catalogs from which individual storms are randomly sampled. Subsequently, frequency analysis can be performed based on consecutive years of randomly transposed storms. The choice of the size of the catalog (the number of storms included) influences the results of the frequency analysis quite significantly. Since the radar dataset we utilize in the present study is incomplete in time, as described in Section 2.4, we choose to create catalogs containing all of the available data and compare them to the available rain-gauge datasets. In Figure 2, we compare ranked domain-average rainfall depths for durations 10, 60, 720, and 1440 min for (1) in black, the 1104 days included in the radar dataset; (2) in orange, the largest 1104 values included in the short-term rain-gauge dataset over the same period covered by the radar data; and (3) in blue, the 1104 days of rain gauge data, which coincide temporally with the radar dataset. The discrepancy between the orange and the blue lines indicates that the radar dataset is abrupt and incomplete, since there are values within the full period of rain-

gauge data which are not included in the rain-gauge dataset, coinciding temporally with the radar dataset. The discrepancy is evident both in the domain-average data (solid lines) and in the single pixel/point data (dashed lines). As described in Section 2.4, the incomplete radar dataset is caused by the removal of defective radar data, days with radar data outages, days with less than 3 mm recorded rain in at least one rain gauge used for bias-adjustment, and the filtering of data with poor bias adjustment over the observation period.

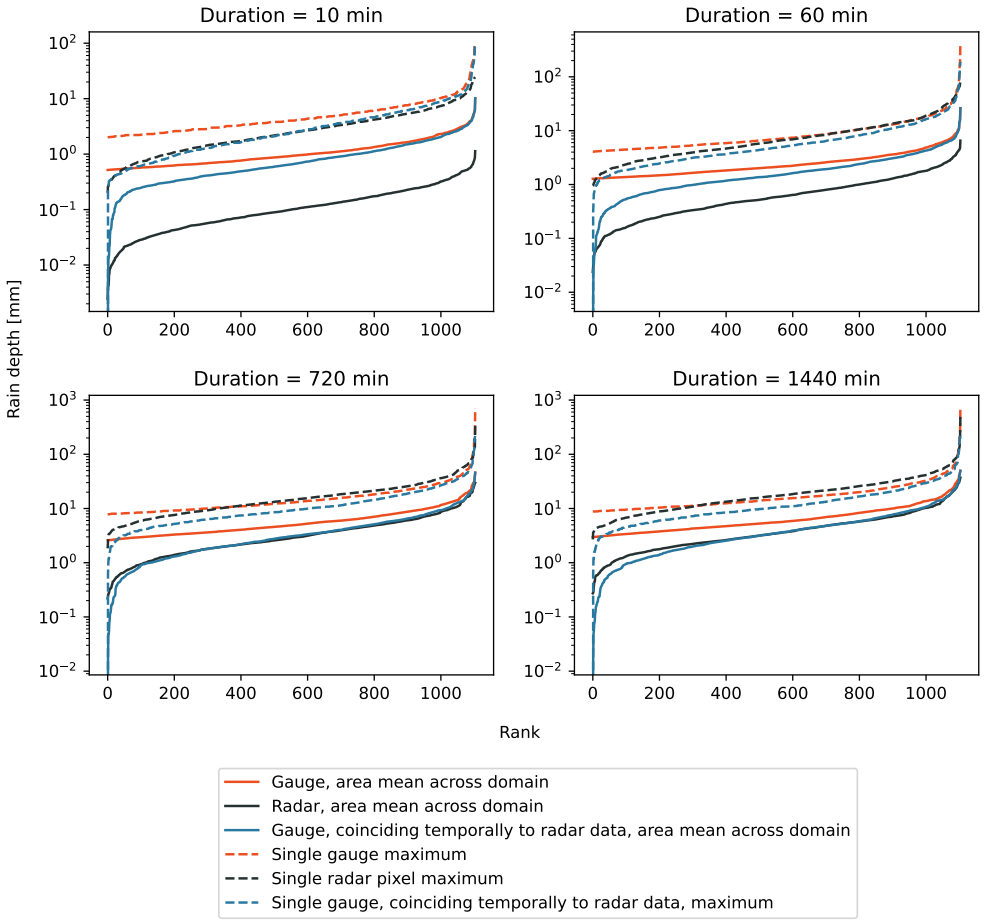

Figure 2. Ranked maximum point (dashed lines) and transposition domain average (solid lines) rainfall depths for short-term rain-gauges (orange) and generated radar-data storm catalogs (black). Blue lines show the short-term gauge dataset adjusted so that the dates coincide with the radar dataset.

Furthermore, the relation between the generated catalogs (black lines, Figure 2) and the gauge data (orange and blue lines, Figure 2), shows a significant discrepancy at short rainfall durations which diminishes with longer durations. This difference is, as also pointed out by Thorndahl et al. [20] and Thomassen et al. [31], a consequence of scaling between point and pixel, which is most predominant at smaller durations. This is often referred to as radar subpixel variability. Similar differences between radar rainfall products and rain gauges have been observed in Peleg et al. [39,41]. While the spatial resolution of the radar data applied in this study is relatively high, the subpixel variability is still a significant factor.

The fact that the radar data is bias-adjusted against rain gauges at daily time scale [30] might also influence the underestimation of short-duration intensities. This is discussed further in Section 4.3, where duration-specific biases are presented.

Another explanation for the differences between radar and gauge data is related to the spatial extent of storms and the difference in estimating areal rainfall from averaging points versus averaging pixels over the domain. Figure 3 shows examples of individual storms from the catalog. The low, median, and high values refer to the ranking based on the areal rainfall

over the whole domain for durations of 10, 60, 720, and 1440 min. Short-duration rainfall events tend to have low spatial extent, which is clearly visible in Figure 3 for the 10-min catalogs. Even the 10-min storm ranked the highest in terms of average-domain depth, has a limited spatial extent, and, therefore, a significant area with near-zero rainfall in the remaining part of the domain. We see less discrepancy between rain-gauge and radar data for longer storm durations due to the temporal smoothing of spatial rainfall variability as a storm passes over a specific area. However, we see that even storms with the longest duration of 1440 min can have a low spatial extent, thus meaning that the number of storms we choose to include in the catalogs can significantly impact the frequency analysis results.

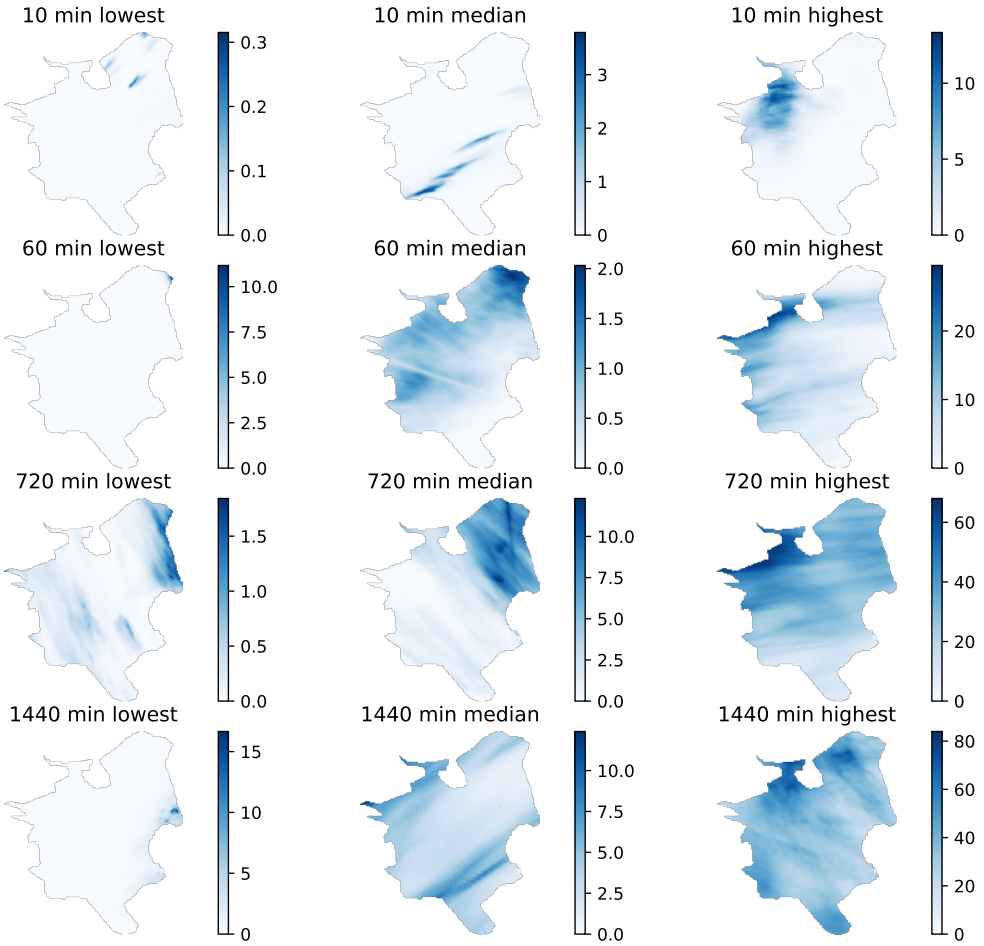

Figure 3. Examples of the spatial variability of accumulated rainfall depths for the duration-specific storms added to the final rainfall catalogs. The unit for the colorbars are in mm rainfall depth. Lowest, median, and highest refer to the rank of the domain mean rainfall depth.

In stochastic transposition, a small spatial extent of storms entails a reduction in the probability of transposing the center of the storm to the area of interest. Likewise, it increases the probability of transposing areas with zero rainfall to the area of interest.

As stated above, the gauge data adjusted to coincide temporally with the radar data, in Figure 2 (blue line), indicates that while the largest storms in each catalog are closely similar to the largest storms of the full rain-gauge dataset, the discrepancy increases with lower rank for the smaller durations. This indicates that, especially, short-duration storms are undersampled in the radar dataset. In order to compensate for this undersampling and small spatial extent for short-duration storms, we need to increase the number of storms we sample per year in the SST procedure. More specifically, this means that we cannot use a similar assumption of estimating the Poisson distributed annual exceedances by $\lambda = \frac{m}{n}$, where m is the number

of storms included in the storm catalog and n is the total period of record, that is used in Wright et al. [24].

Instead, we estimate the λ parameter by (1) choosing a specific number of storms exceedances for each catalog to include in the analysis, (2) looking up the domain average radar rainfall corresponding to that number of exceedances (solid black line, Figure 2), and (3) determining the corresponding number of exceedances in the area mean rain-gauge dataset (solid orange line, Figure 2). As an example: the 100 largest storms from the radar dataset yields a $\lambda \approx 35$ yrs^{-1} instead of $\lambda \approx 6$ yrs^{-1} ($\lambda = \frac{100}{17\,\mathrm{yrs}}$).

The adjusted λ value, which we use as a key parameter in SST sampling, is estimated as an average for all durations. Due to the significantly lower domain average values, the 10-minute catalog tends to give larger λ values regardless of the number of storms included in the catalog. Using only the largest storms, e.g., 100, will lead to an oversampling of the storms in the catalog, which might skew the frequency analysis results. To prevent oversampling, we select a total of the 500 largest storms to be included in each catalog since we observe stationarity in the output of the frequency analysis with this number of storms (not shown). This specific study leads us to use a λ value equal to 88 for the SST frequency analysis. $\lambda = 88$ yr^{-1} should be considered a parameter optimized for this specific radar dataset to compensate for missing data and the small spatial extents of short-duration storms. The value is, thus, not directly comparable to the annual number of storm occurrences as applied in other studies, e.g., in Wright et al. [24].

4.3. IDF Curves Based on Empirical Plotting Position, Extreme-Value Distribution Fit, and Comparison to SST

In this section, we compare IDF curves derived from rain-gauge and radar data at point/pixel scale using the PDS (plotting position ranking) and GPD fit approaches (Section 3.2) and compare them to the derived IDF curves based on the SST approach. This comparison is central in studying the relation between return level and data observation period and the consequent limits in the frequency analysis for short observation series. In this case, the radar data observation covers 17 full years (2002–2019) and merits an empirical frequency analysis for low return levels (e.g., 1, 2, or 5 years).

The PDS and empirical plotting-position approaches are used to estimate return levels for mean rainfall intensities at the durations of 10, 30, 60, 180, 360, 720, and 1440 min. Figure 4 shows the frequency analysis for a 60-minute and a 1440-minute rainfall duration, for a single rain gauge (see Figure 1, long-term gauge, adjusted to cover same period of record as the radar) and the corresponding radar pixel. For comparison, the ranked values generated by the SST procedure are shown on a linear axis (left) and a log axis (right) extending to 1000-year return levels.

Figure 4 shows that the GPD model with the ensemble spread encapsulates the ranked observed 60-min and 1440-min intensities for both the rain-gauge and radar datasets. In general, the observed extremes agree with the estimated mean values from the GPD. Return levels above 5 years display more significant statistical uncertainty, which is to be expected for this relatively short period of record.

Figure 4, furthermore, shows a significant difference between the rain-gauge and radar datasets. For both observed values and GPD fit, radar-based results underestimate the intensities compared to the rain-gauge values. This underestimation is most predominant for the 60-min values and is caused by the same challenges in point/pixel comparisons for short durations as described in Section 4.2. In comparison, Thorndahl et al. [20] report an average difference of 15% (over a large dataset) due to this scaling error and we observe a bias of 19% according to the values in Table 1 for rainfall durations of 60 min. It is, however, evident from both this study as well as Schleiss et al. [9] and Thomassen et al. [31] that the scaling error can be significantly larger in extreme-value analysis. This is also supported by Wright et al. [42], who state that errors such as these tend to be heteroscedastic, meaning that the magnitude of error is dependent on rainfall intensity [43] and has been shown to increase with rainfall intensity [44].

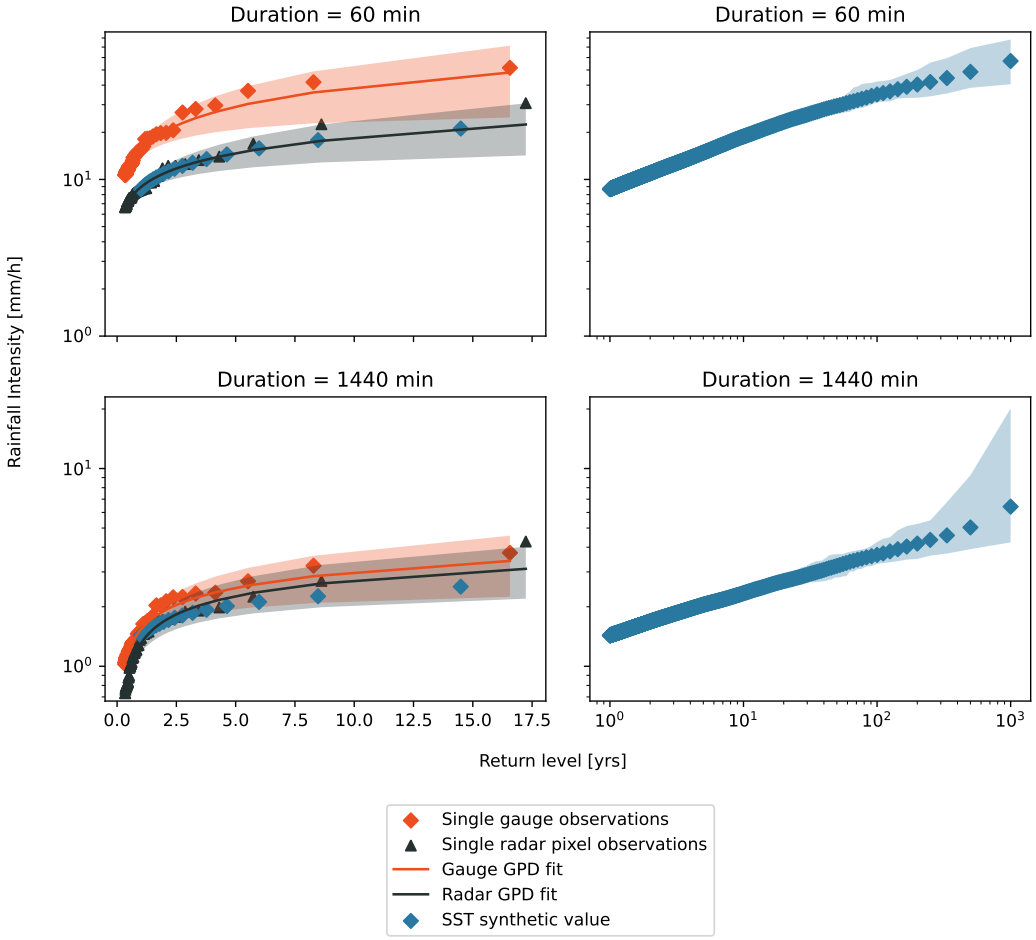

Figure 4. GPD-based frequency analysis for long-term gauge (orange) and the corresponding radar pixels (black). The lines indicate the fitted GPD-model and shaded area depicts model uncertainty. Ranked values of synthetic rainfall years generated by the SST procedure are also shown (blue). Due to the high density of points, only every 50th SST point is shown on the figures to the left.

The scaling discrepancy can also be seen in Figure 5, where we show IDF-curves for return levels of 2, 5, and 10 years for all of the short-term gauges (Figure 1, 2002–2019) and their corresponding radar pixels. The curves are derived using the PDS approach, and return levels are estimated from Equation (1). The uncertainty bands explain the discrepancies between the different gauges/pixels included in the datasets. They are, thus, a measure of both spatial variabilities and the stochastic nature of rainfall. In this case, we also see heteroscedasticity, i.e., larger variability for increasing intensity. The overall bias between the two datasets also increases as the rainfall intensity increases, as shown above for the long-term datasets and shown in Figure 6 and Table 1.

Table 1. Bias, root mean square error (RMSE) and mean absolute error (MAE) for all investigated rainfall durations.

Rainfall Duration [min]	**10**	**30**	**60**	**180**	**360**	**720**	**1440**
Bias [-]	1.56	1.27	1.19	1.11	1.06	1.03	1.00
RMSE [mm]	8.71	4.43	3.09	1.42	0.83	0.47	0.25
MAE [mm]	4.49	2.28	1.46	0.69	0.41	0.23	0.12

The biases between the radar and rain-gauge values are likely the cause of the sub-hourly differences for the IDF estimates presented and discussed in Section 4.4, Figure 7.

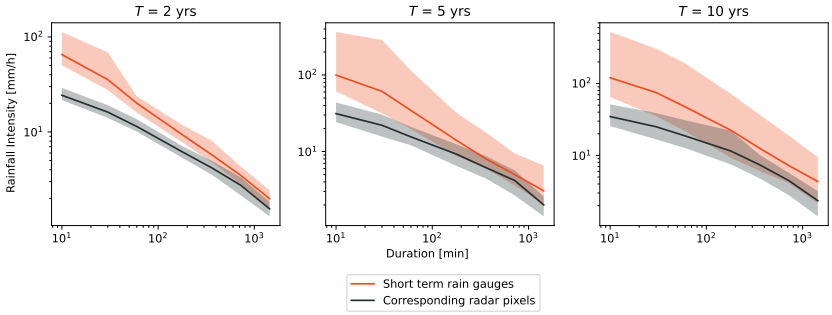

Figure 5. IDF-curves for all of the short-term rain gauges (orange) and their corresponding radar pixels (black). The solid line indicates median values and the shaded area depicts the total ensemble spread between gauges. The curves represent return levels of 2, 5, and 10 years.

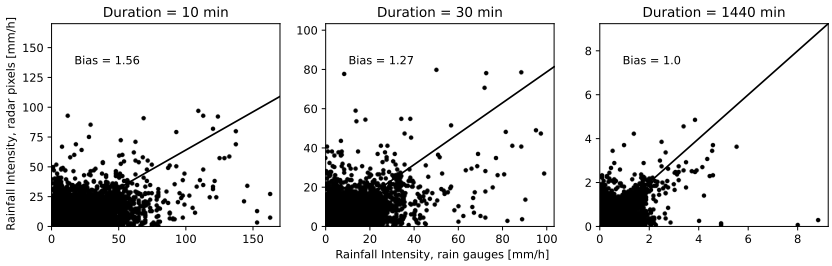

Figure 6. Biases for duration of 10, 30, and 1440 min. Biases are calculated by Equation (4).

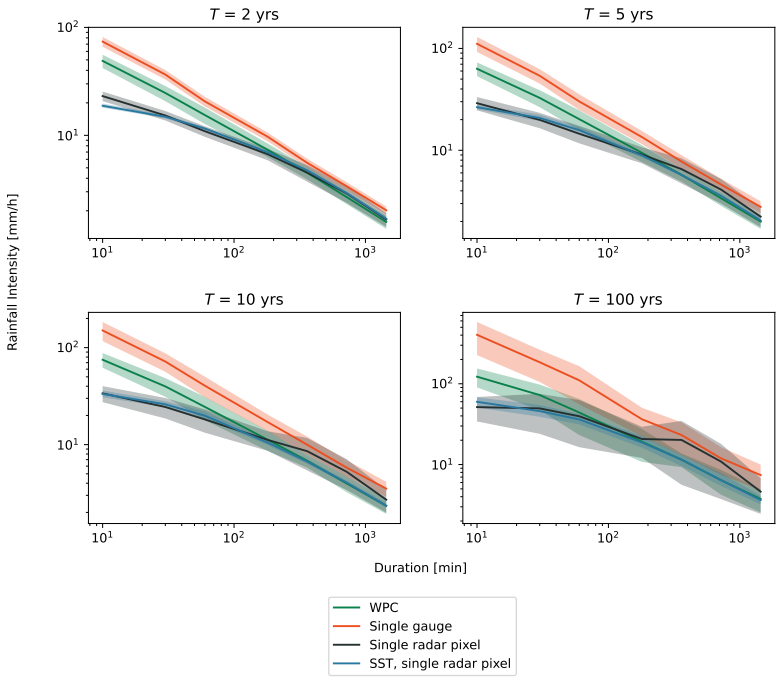

Figure 7. IDF-curves (10 min to 1440 min) for the regional model (green, WPC); long-term rain gauge, derived from GPD fit (orange); single radar pixel, derived from GPD fit (black, Radar), and the SST framework (blue, SST). The shaded area depicts 95% confidence interval, and total ensemble spread for SST values. Each curve represents a return level of: 2, 5, 10, and 100 years.

It should be noted that while the above analysis shows significant bias towards the rain gauges, especially at short rainfall durations, a more precise IDF estimation would not necessarily be achieved by adjusting the storm catalogs by the presented biases. Even at low return levels, such as T = 2 years, we observe quite a significant uncertainty (Figure 5) in

the hourly/sub-hourly extreme rain rates and a final ground truth possibly lies somewhere between the radar- and rain-gauge-derived extreme values.

4.4. Point-to-Pixel Comparison of IDF Curves

In this section, we compare the SST-derived IDF relationships to the IDF-relationships of the danish regional model (WPC) at point/pixel scale. For comparison reasons, we maintain the GPD-fitted IDF values from the long-term gauge and corresponding radar pixel from Section 4.3, since the GPD-fit allows us to extrapolate to return levels extending beyond the observation period. Figure 7 shows IDF curves at return levels: 2, 5, 10, and 100 years for durations from 10 to 1440 min.

The SST procedure generates IDF curves very similar to that of the GPD derived from the single-pixel radar dataset, showing that the methodology can produce rainfall statistics comparable to traditional methods. The radar-based values (blue and black lines in Figure 7) both underestimate, at short rainfall duration (sub 180 min), when compared to rain-gauge-based IDF curves (orange and green line, Figure 7). This is in-line with studies of the same radar dataset [20,30,31] and also from what is presented in Figures 4 and 5. Above the 180-minute duration, the IDF curves are more or less in agreement. The single-gauge-based IDF curves (orange line, Figure 7) overestimate across durations and return levels indicating that this single rain gauge, in general, registered more extreme rainfall, a trend we also observe in Figure 5.

A clear advantage of the SST framework is its stability to statistical certainty. For return levels of 10 and 100 years, we see the SST-derived values have a much narrower ensemble spread and more overall stability across the durations than the other datasets. Bearing in mind that the observation period of the radar dataset, from which the SST values are generated, is significantly shorter than the single-gauge dataset and the dataset underlying the WPC-values, this is an essential result. It proves that we, in fact, can produce comparable statistics by transposing spatial rainfall from the domain to the point of interest.

One of the limitations or even disadvantages of the SST framework is noticeable at the 10-minute duration and most significantly at the 2-year return level, Figure 7. Compared to the radar data, the SST procedure underestimates the intensities. This is most likely because of how the spatio-temporal sampling is executed. As elaborated in [24,25,34] and also visible in Figures 2 and 3, short-duration storms have a very low spatial extent. This will result in sampling a significant portion of zero values and, thus, skewing the frequency analysis. Wright et al. [24] suggest increasing the number of included storms and the number of storms sampled per year. However, this study shows that the effect of increased sampled storms is negligible, potentially due to oversampling. A different solution could be to update the SST framework such that a non-uniform spatial-transposition scheme for each of the included storm durations is implemented. Potentially, this could lower the number of zero values sampled and, thus, result in a non-skewed frequency analysis. In the complete radar dataset, we do in fact have max. values, across all durations, similar to max. values of a rain-gauge-based dataset, and it is, to some extent, a matter of transposition. RainyDay [34] does offer a non-uniform transposition scheme based on the geographical occurence of the maximum point for the applied storm catalog. This feature was implemtented in this study (not shown) but showed very negliable effetcts. This transposition scheme is not able to account for the short areal extent of short-duration storms, as presented in Figure 3, and will still result in transposing zero rainfall over the area of interest.

The scaling issues between point and pixel at short rainfall durations are, nonetheless, unavoidable and should not be compensated by adapting the SST framework. The latter advocates for one of the real advantages of the SST framework, namely, to generate extreme-value statistics at catchment scale rather than point scale. This is studied in the following section.

4.5. Catchment-Scale Comparison of IDF Curves

Having the validity of the SST framework investigated and confirmed in Section 4.4, we present a similar analysis, in Figure 8, for IDF curves at catchment scale using the same types of rainfall data. In order to go from point scale to catchment scale, the following modifications are made to the rainfall data:

- ARFs are applied to the regional model (WPC) using Equation (5).
- The collection of medium-term rain gauges (Figure 1) is used to create an area-mean rainfall time series, from which the GPD model is fitted, representing the area of interest (AOI); see Figure 1.
- Radar pixels within the AOI are, likewise, used to create an area-mean rainfall time series, and a GPD model is fitted, albeit with significantly more data points than the collection of gauges.
- Instead of only sampling one point for the SST framework, all points within the AOI are used to calculate a catchment average for the randomly generated rainfall event.

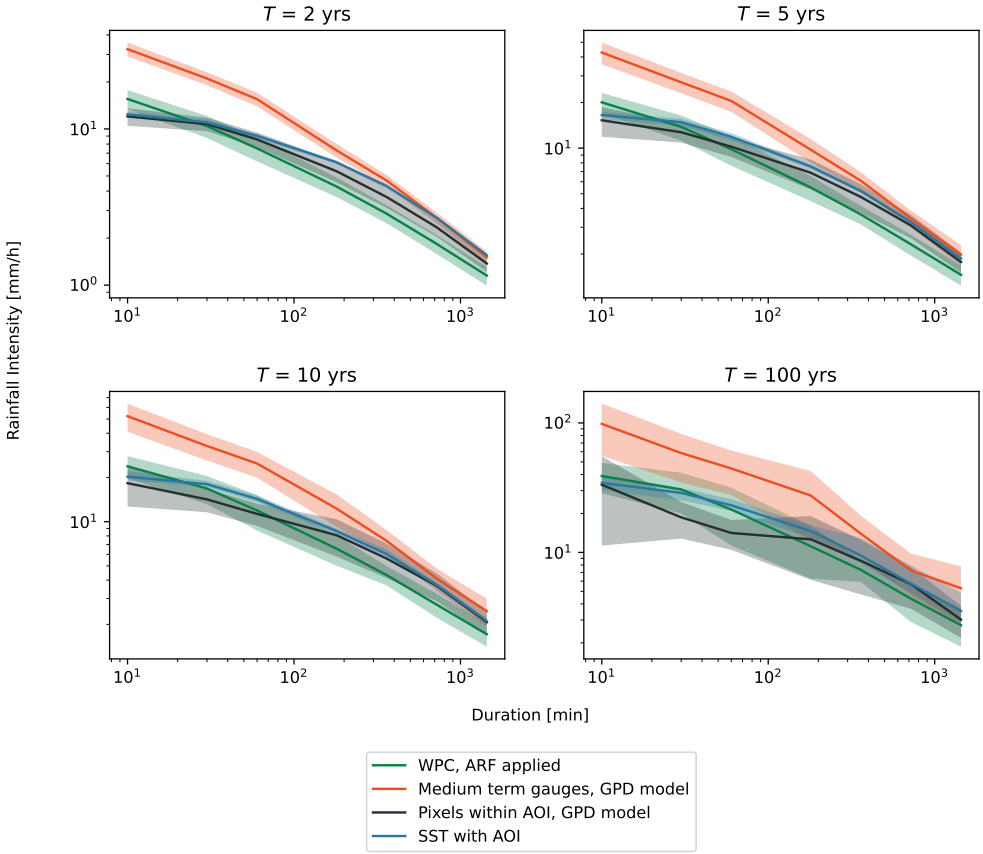

Figure 8. IDF curves (10 min to 1440 min) for the regional model with ARFs applied (green, WPC); collection of medium-term gauges, derived from GPD fit (orange, Gauge); radar pixels within the AOI, derived from GPD fit (black, Radar) and the SST framework for AOI (blue, SST). Shaded area depicts 95% confidence interval and total ensemble spread for SST values. Each curve is representing a return level of: 2, 5, 10 and 100 years.

The SST framework performs on a par with traditional methods, as is evident by an overall agreement between the GPD model fitted to the radar data and the results of the SST framework (black and blue line, in Figure 8, respectively). The SST framework overestimates intensities slightly compared to the base radar data. This is also expected, since the base radar data is fixed to one spatial area and consists of a relatively short time series. The SST framework samples values from a much larger domain area and virtually creates rainfall for 1000 years, thus resulting in slightly higher values.

Similarly, we observe a general agreement between the regional model and the two radar-based IDF-curves, albeit with significant discrepancies at long rainfall durations. A common criticism and general flaw [21] of the ARF approach is the negligence of the rainfall fields' structure and return levels of the area in question. This statement is supported by the examples of 5-year storms presented in Figure 9. While the catchment average rainfall intensity for all three storms is the same and equivalant to the 5-year return level and a 1440-min duration, they all have vastly different spatio-temporal structures.

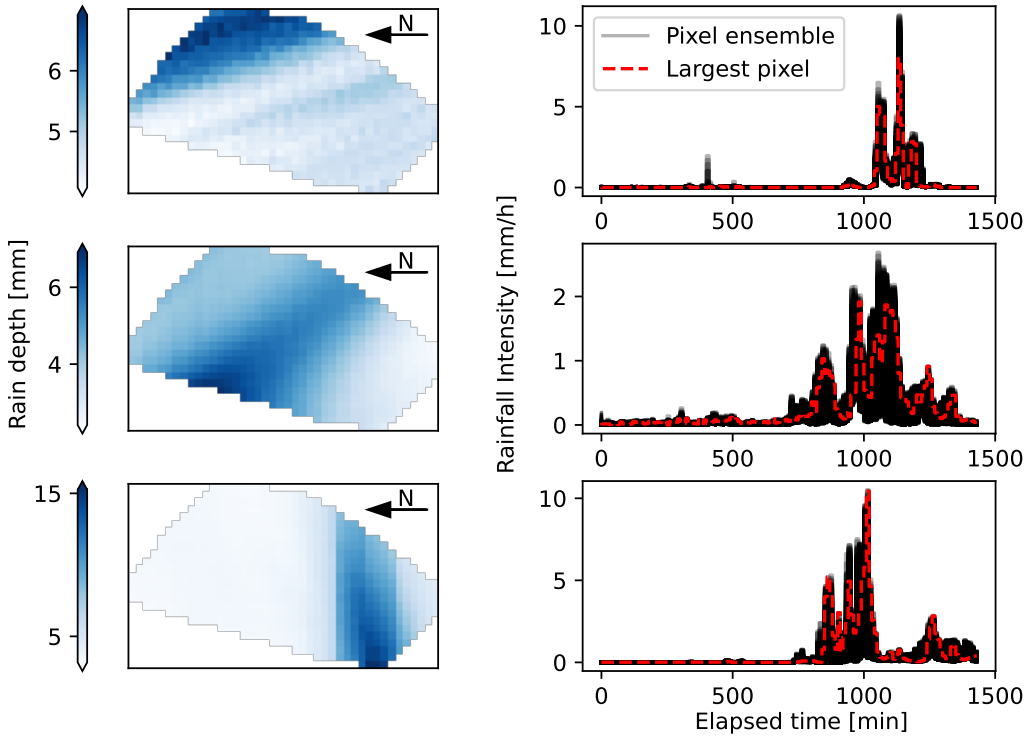

Figure 9. Generated 5-year storms for a duration 1440 min, shown on the left. The storms was arbitrarily selected. On the right, time series for each individual pixel is shown (black) and the largest pxiel based on accumulated rain depth (dashed red line).

The IDF curves derived from the collection of medium-term rain gauges overestimate, relative to the other IDF curves, for most of the rainfall durations. Rainfall fields exhibit a characteristic scaling nature where (1) the rainfall extremes are sensitive to the overall scale [45] and (2) the spatial structure itself can, likewise, vary significantly [24]. By constructing a catchment-scale time series based on five points only, the frequency analysis shows overestimation since the complex structure of the rainfall fields are neglected.

Figure 9 highlights one of the advantages of the SST framework: the ability to identify specific catchment-area rainfall events and classify their return levels, allowing for a much more detailed analysis of hydrological infrastructure. For complex surface areas such as urban environments, the presented storms (Figure 9) will most likely result in vastly different response signals. The relation between stochastically transposed areal input and system response is an objective to further investigate in another study.

5. Conclusions

In this study, we apply the SST framework to a discontinuous radar dataset to derive IDF curves for sub-hourly to daily, low-return-level rainfall durations. These SST-based IDF curves are compared to traditionally derived IDF curves from long rain-gauge records, a regional extreme-value model based on rain gauges, and untransposed radar data. For point rainfall, we find that the SST framework using radar data can produce IDF curves similar to the traditionally derived IDF curves based on a significantly shorter data period. In this way,

the stochastic transposition utilizes the spatial variability of rainfall within the studied domain to derive extreme-value statistics. It can, therefore, estimate valid return levels larger than the observation period. Due to scaling issues between point and pixel scale, the derived SST values underestimate rainfall intensities at short rainfall durations of less than 180 min. Still, this discrepancy is more related to the properties of the radar data rather than an actual problem with the SST framework. The results broadly follow the conclusions of Wright et al. [24], however, with a different dataset with sub-hourly discretization, a finer spatial resolution, and in a different climatological region. We show that even with an incomplete radar dataset of approx. 1100 recorded rainfall days over 17 years, the SST framework still recreates IDF curves comparable to that of traditionally derived methods when sampling parameters are adjusted to account for missing data.

The SST framework shows great promise as a design and risk-assessment tool by increasing our understanding of the spatio-temporal dynamics of rainfall fields. The ability to generate rainfall events and assign return levels at catchment scale allows modelers and decision makers to investigate hydrological- and hydraulic-system responses. The impacts of spatio-temporal rainfall variability can, therefore, be studied in detail, especially in urban areas where the spatial heterogeneity of surface area tends to be significant.

Author Contributions: Conceptualization, C.B.A. and D.B.W.; methodology, C.B.A. and D.B.W.; software, C.B.A. and D.B.W.; validation, C.B.A. and S.T.; formal analysis, C.B.A.; investigation, C.B.A.; resources, S.T.; data curation, C.B.A. and S.T.; writing—original draft preparation, C.B.A.; writing—review and editing, D.B.W. and S.T; visualization, C.B.A.; supervision, S.T. and D.B.W.; project administration, S.T.; funding acquisition, S.T. All authors have read and agreed to the published version of the manuscript.

Funding: This work is partly funded by VUDP, DANVA, Denmark grant no. 1162.2017 and Aarhus Water Utility, Denmark.

Data Availability Statement: Restrictions apply to the availability of the rain gauge data from WPC and for the radar data from DMI.

Acknowledgments: The authors would like to acknowledge the Danish Meteorological Institute (DMI) and the Danish Water Pollution Committee (WPC) within IDA: The Danish Society of Engineers for the use of radar and rain gauge data.

Conflicts of Interest: The authors declare no conflict of interest.

References

1. Madsen, H.; Arnbjerg-nielsen, K.; Mikkelsen, P.S. Update of regional intensity–duration–frequency curves in Denmark: Tendency towards increased storm intensities. *Atmos. Res.* **2009**, *92*, 343–349. [CrossRef]
2. Madsen, H.; Mikkelsen, P.S.; Rosbjerg, D.; Harremoës, P. Regional estimation of rainfall intensity-duration-frequency curves using generalized least squares regression of partial duration series statistics. *Water Resour. Res.* **2002**, *38*, 21-1–21-11. [CrossRef]
3. Cristiano, E.; ten Veldhuis, M.; van de Giesen, N. Spatial and temporal variability of rainfall and their effects on hydrological response in urban areas—A review. *Hydrol. Earth Syst. Sci.* **2017**, *21*, 3859–3878. [CrossRef]
4. Kim, C.; Kim, D. Effects of Rainfall Spatial Distribution on the Relationship between Rainfall Spatiotemporal Resolution and Runoff Prediction Accuracy. *Water* **2020**, *12*, 846. [CrossRef]
5. Courty, L.; Rico-Ramirez, M.; Pedrozo-Acuña, A. The Significance of the Spatial Variability of Rainfall on the Numerical Simulation of Urban Floods. *Water* **2018**, *10*, 207. [CrossRef]
6. Ochoa-rodriguez, S.; Wang, L.; Gires, A.; Pina, R.D.; Reinoso-Rondinel, R.; Bruni, G.; Ichiba, A.; Gaitan, S.; Cristiano, E.; van Assel, J.; et al. Impact of spatial and temporal resolution of rainfall inputs on urban hydrodynamic modelling outputs: A multi-catchment investigation. *J. Hydrol.* **2015**, *531*, 389–407. [CrossRef]
7. Gyasi-Agyei, Y. Identification of the Optimum Rain Gauge Network Density for Hydrological Modelling Based on Radar Rainfall Analysis. *Water* **2020**, *12*, 1906. [CrossRef]
8. Einfalt, T.; Arnbjerg-Nielsen, K.; Golz, C.; Jensen, N.; Quirmbach, M.; Vaes, G.; Vieux, B. Towards a roadmap for use of radar rainfall data in urban drainage. *J. Hydrol.* **2004**, *299*, 186–202. [CrossRef]
9. Schleiss, M.; Olsson, J.; Berg, P.; Niemi, T.; Kokkonen, T.; Thorndahl, S.; Nielsen, R.; Nielsen, J.E.; Bozhinova, D.; Pulkkinen, S. The accuracy of weather radar in heavy rain: A comparative study for Denmark, the Netherlands, Finland and Sweden. *Hydrol. Earth Syst. Sci.* **2019**, *24*, 3157–3188. [CrossRef]

10. Thorndahl, S.; Einfalt, T.; Willems, P.; Nielsen, J.E.; ten Veldhuis, M.; Arnbjerg-Nielsen, K.; Rasmussen, M.R.; Molnar, P. Weather radar rainfall data in urban hydrology. *Hydrol. Earth Syst. Sci.* **2017**, *21*, 1359–1380. [CrossRef]
11. Overeem, A.; Buishand, T.A.; Holleman, I.; Uijlenhoet, R. Extreme value modeling of areal rainfall from weather radar. *Water Resour. Res.* **2010**, *46*. [CrossRef]
12. Schaefer, M.G. Regional analyses of precipitation annual maxima in Washington State. *Water Resour. Res.* **1990**, *26*, 119–131. [CrossRef]
13. Madsen, H.; Rasmussen, P.F.; Rosbjerg, D. Comparison of annual maximum series and partial duration series methods for modeling extreme hydrologic events: 1. At-site modeling. *Water Resour. Res.* **1997**, *33*, 747–757. [CrossRef]
14. Madsen, H.; Rosbjerg, D. Generalized least squares and empirical bayes estimation in regional partial duration series index-flood modeling. *Water Resour. Res* **1997**, *33*, 771–781. [CrossRef]
15. Keifer, C.J.; Chu, H.H. Synthetic Storm Pattern for Drainage Design. *J. Hydr. Eng. Div. ASCE* **1957**, *83*, 1332-1–1332-25. [CrossRef]
16. Rosbjerg, D.; Madsen, H. Initial design of urban drainage systems for extreme rainfall events using intensity-duration-area (IDA) curves and Chicago design storms (CDS). *Hydrol. Sci. J.* **2019**, *64*, 1397–1403. [CrossRef]
17. Sivapalan, M.; Blöschl, G. Transformation of point rainfall to areal rainfall: Intensity-duration-frequency curves. *J. Hydrol.* **1998**, *204*, 150–167. [CrossRef]
18. Rodriguez-iturbe, I.; Mejía, J. On the transformation of point rainfall to areal rainfall. *Water Resour. Res.* **1974**, *10*, 729–735. [CrossRef]
19. Allen, R.J.; Degaetano, A.T. Considerations for the use of radar-derived precipitation estimates in determining return intervals for extreme areal precipitation amounts. *J. Hydrol.* **2005**, *315*, 203–219. [CrossRef]
20. Thorndahl, S.; Nielsen, J.E.; Rasmussen, M. Estimation of Storm-Centred Areal Reduction Factors from Radar Rainfall for Design in Urban Hydrology. *Water* **2019**, *11*, 1120. [CrossRef]
21. Wright, D.B.; Smith, J.A.; Baeck, M.L. Critical Examination of Area Reduction Factors. *J. Hydrol. Eng.* **2014**, *19*, 769–776. [CrossRef]
22. Foufoula-Georgiou, E. A probabilistic storm transposition approach for estimating exceedance probabilities of extreme precipitation depths. *Water Resour. Res.* **1989**, *25*, 799–815. [CrossRef]
23. Wilson, L.L.; Foufoula-Georgiou, E. Regional Rainfall Frequency Analysis via Stochastic Storm Transposition. *J. Hydraul. Eng. ASCE* **1990**, *116*, 859–880. [CrossRef]
24. Wright, D.B.; Smith, J.A.; Villarini, G.; Baeck, M.L. Estimating the frequency of extreme rainfall using weather radar and stochastic storm transposition. *J. Hydrol.* **2013**, *488*, 150–165. [CrossRef]
25. Wright, D.B.; Smith, J.A.; Baeck, M.L. Flood frequency analysis using radar rainfall fields and stochastic storm transposition. *Water Resour. Res.* **2014**, *50*, 1592–1615. [CrossRef]
26. Heiss, W.H.; McGrew, D.L.; Sirmans, D. Nexrad: Next generation weather radar (WSR-88D). *Microw. J.* **1990**, *33*, 79.
27. *Opdaterede klimafaktorer og dimensionsgivende regnintensiteter Spildevandskomiteen, Skrift nr. 30 (Updated Climate Factors and Design Rainfall Intensityes Water Pollution Comitee, Guideline no. 30)*; The Water Pollution Committee of the Society of Danish Engineers, IDA: Copenhagen, Denmark, 2007.
28. Madsen, H.; Gregersen, I.B.; Rosbjerg, D.; Arnbjerg-Nielsen, K. Regional frequency analysis of short duration rainfall extremes using gridded daily rainfall data as co-variate. *Water Sci. Technol.* **2017**, *75*, 1971–1981. [CrossRef]
29. Gregersen, I.B.; Madsen, H.; Rosbjerg, D.; Arnbjerg-Nielsen, K. A spatial and nonstationary model for the frequency of extreme rainfall events. *Water Resour. Res.* **2013**, *49*, 127–136. [CrossRef]
30. Thorndahl, S.; Nielsen, J.E.; Rasmussen, M.R. Bias adjustment and advection interpolation of long-term high resolution radar rainfall series. *J. Hydrol.* **2014**, *508*, 214–226. [CrossRef]
31. Thomassen, E.D.; Thorndahl, S.; Andersen, C.B.; Gregersen, I.B.; Arnbjerg-Nielsen, K.; Sørup, H.J.D. Comparing spatial metrics of extreme precipitation between data from rain gauges, weather radar and high-resolution climate model re-analyses. *J. Hydrol.* **2022**, *610*, 127915. [CrossRef]
32. Nielsen, J.E.; Thorndahl, S.; Rasmussen, M.R. A numerical method to generate high temporal resolution precipitation time series by combining weather radar measurements with a nowcast model. *Atmos. Res.* **2014**, *138*, 1–12. [CrossRef]
33. Thejll, P.; Boberg, F.; Schmith, T.; Christiansen, B.; Christensen, O.B.; Madsen, M.S.; Su, J.; Andree, E.; Olsen, S.; Langen, P.L.; et al. *Methods Used in the Danish Climate Atlas*; DMI Report 21-41; Danish Meteorological Institute: Copenhagen, Denmark, 2021; ISBN 978-87-7478-690-0.
34. Wright, D.B.; Mantilla, R.; Peters-Lidard, C.D. A remote sensing-based tool for assessing rainfall-driven hazards. *Environ. Model. Softw.* **2017**, *90*, 34–54. [CrossRef]
35. Zhou, Z; Smith, J.A.; Baeck, M.L.; Wright, D.B.; Smith, B K.; Liu, S. The impact of the spatiotemporal structure of rainfall on flood frequency over a small urban watershed: An approach coupling stochastic storm transposition and hydrologic modeling. *Hydrol. Earth Syst. Sci.* **2021**, *25*, 4701–4717. [CrossRef]
36. Zhu, Z.; Wright, D.B.; Yu, G. The Impact of Rainfall Space-Time Structure in Flood Frequency Analysis. *Water Resour. Res.* **2018**, *54*, 8983–8998. [CrossRef]
37. WPC. *Funktionspraksis for afløbssystemer under regn, skrift nr. 27 (Practice for Drainage Systems during Rain, Guideline no. 27)*; The Water Pollution Committee of the Society of Danish Engineers, IDA: Copenhagen, Denmark, 2007.
38. Willems, P.; Olsson, J.; Arnbjerg-Nielsen, K.; Beecham, S.; Pathirana, A.; Gregersen, IB.; Madsen, H.; Nguyen, V.-T.-V. *Impacts of Climate Change on Rainfall Extremes and Urban Drainage Systems*; IWA Publishing: London, UK, 2012; ISBN 9781780401263.

39. Peleg, N.; Marra, F.; Fatichi, S.; Paschalis, A.; Molnar, P.; Burlando, P. Spatial variability of extreme rainfall at radar subpixel scale. *J. Hydrol.* **2018**, *556*, 922–933. [CrossRef]
40. Scharling, M. *Climate Grid Denmark—Dataset for Use in Research and Education*; Technical Report 12-10; Danish Meteorological Institute: Copenhagen, Denmark, 2012.
41. Peleg, N.; Ben-asher, M.; Morin, E. Radar subpixel-scale rainfall variability and uncertainty: Lessons learned from observations of a dense rain-gauge network. *Hydrol. Earth Syst. Sci.* **2013**, *17*, 2195–2208. [CrossRef]
42. Wright, D.B.; Kirschbaum, D.B.; Yatheendradas, S. Satellite Precipitation Characterization, Error Modeling, and Error Correction Using Censored Shifted Gamma Distributions. *J. Hydrometeorol.* **2017**, *18*, 2801–2815. [CrossRef]
43. Ciach, G.J.; Morrissey, M.L.; Krajewski, W.F. Conditional Bias in Radar Rainfall Estimation. *J. Appl. Meteorol.* **2000**, *39*, 1941–1946. [CrossRef]
44. Tian, Y.; Huffman, G.J.; Adler, Robert F.; Tang, L.; Sapiano, M.; Maggioni, V.; Wu, H. Modeling errors in daily precipitation measurements: Additive or multiplicative? *Geophys. Res. Lett.* **2013**, *40*, 2060–2065. [CrossRef]
45. Bougadis, J.; Adamowski, K. Scaling model of a rainfall intensity-duration-frequency relationship. *Hydrol. Process.* **2006**, *20*, 3747–3757. [CrossRef]